Journal of Atmospheric and Solar-Terrestrial Physics 73 (2011) 1129–1137

Contents lists available at ScienceDirect

Journal of Atmospheric and Solar-Terrestrial Physics

journal homepage: www.elsevier.com/locate/jastp

Rolling motion in erupting prominences observed by STEREO

Olga Panasenco [a,*], Sara Martin [a], Anand D. Joshi [b], Nandita Srivastava [b]

[a] Helio Research, La Crescenta, CA, USA
[b] Udaipur Solar Observatory, Physical Research Laboratory, Udaipur, India

ARTICLE INFO

Article history:
Received 2 April 2010
Received in revised form
19 August 2010
Accepted 3 September 2010
Available online 19 September 2010

Keywords:
Sun: chromosphere
Sun: corona
Sun: filaments
Sun: magnetic fields
Sun: photosphere
Sun: prominences

ABSTRACT

We analyze the large-scale dynamical forms of three erupting prominences (filaments) observed by at least one of the two STEREO spacecraft and which reveal evidence of sideways rolling motion beginning at the crest of the erupting filament. We find that all three events were also highly non-radial and occurred adjacent to large coronal holes. For each event, the rolling motion and the average non-radial outward motion of the erupting filament and associated CME were away from a neighboring coronal hole. The location of each coronal hole was adjacent to the outer boundary of the arcade of loops overlying the filaments. The erupting filaments were all more non-radial than the CMEs but in the same general direction. From these associations, we make the hypothesis that the degree of the roll effect depends on the level of force imbalances inside the filament arcade related to the coronal hole and the relative amount of magnetic flux on each side of the filament, while the non-radial motion of the CME is related to global magnetic configuration force imbalances. Our analyses of the prominence eruption best observed from both STEREO-A and STEREO-B shows that its spine retained the thin ribbon-like topology that it had prior to the eruption. This topology allows bending, rolling, and twisting during the early phase of the eruption.

1. Introduction

During prominence eruptions with the roll effect (Martin, 2003), the top of the prominence spine is observed to gradually bend to one side of the spine. This sideways rolling creates twist of opposite sign in the two prominence legs as the prominence continues to ascend. The twist is observed to propagate down each leg (Martin, 2003). The roll effect does not occur in all erupting prominences. However, whenever observed, the roll effect gives us essential information and insight into the three-dimensional structure of some classic observed forms of erupting prominences (Panasenco and Martin, 2008).

Before eruption, essentially all prominence spines have the shape of a narrow, thin ribbon with horizontal threads that bend to become nearly vertical at the ends of the spine. In many Hα observations of quiescent prominences, especially when observed against the solar disk, the spine is not visible, but this description remains valid for prominences observed in 304 Å images (Wang et al., 1998).

To learn more about the roll effect we studied three examples of this dynamic effect in large quiescent prominences observed to erupt above the solar limb in images from the EUVI telescope at 304 Å on the STEREO spacecraft. In one case the prominence eruption was observed by both STEREO A and B. In another example, the prominence eruption was observed only by one of the spacecraft STEREO-B. A third event was observed by STEREO-B and only observed in a few frames from STEREO-A. These three events occurred during solar minimum, i.e. at a time when the Sun displayed very low activity. A description of the eruptions, their associated CMEs and circumstances of their magnetic field environment are presented here.

2. Examples of the roll effect in erupting prominences observed by STEREO

2.1. 2008 December 12

The trajectories in Fig. 1 are of the outer boundaries of the erupting prominence of December 12, 2008 (shown as green lines) and its associated CME (shown by red lines) as seen, respectively, by STEREO-A/EUV 304 Å and STEREO-A/COR1 instruments in the SECCHI suite on board the twin STEREO spacecraft (Howard et al., 2008). These concurrent parts of the eruptive event were conspicuously non-radial as seen at the north-east limb from STEREO-A (Figs. 1 and 2).

In Fig. 1, we superposed outlines of the outer boundaries of the CME and the bright core of the prominence plasma for the different moments during the eruption (as observed by STEREO-A EUVI 304 Å and STEREO-A/COR1, respectively). The non-radial

* Corresponding author.
E-mail address: olgapanasenco@aol.com (O. Panasenco).

1364-6826/$ - see front matter © 2010 Elsevier Ltd. All rights reserved.
doi:10.1016/j.jastp.2010.09.010

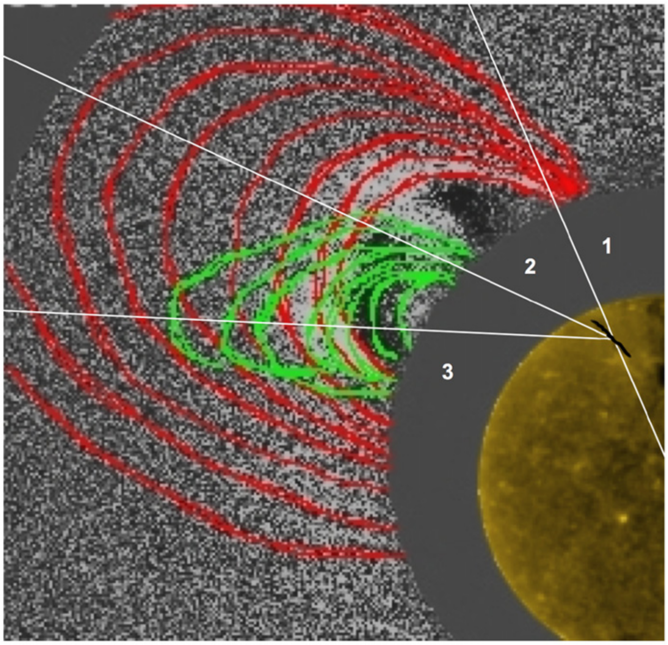

Fig. 1. Non-radial eruption on 2008 December 12. Superposition of the outer boundaries of the CME (red lines) and the erupting prominence inside (green lines) as observed by STEREO-A/COR1 during different moments of the eruption: 07:05, 07:25, 07:45, 08:05, 08:25, 08:45, 09:05 and 09:25 UT. The contour of the filament before eruption is shown by the black line on an image from STEREO-A/EUVI 284 Å. Lines 1, represents the radial line from the prominence site; lines 2 and 3 show the apparent directions of propagation of the CME and erupting prominence, respectively.

propagation is different for the prominence and corresponding CME. The deviation of the CME from the radial propagation is about 40° (the angle between lines 1 and 2) and the difference between the prominence and CME central direction of the eruption is about 20° (the angle between lines 2 and 3).

The erupting prominence is shown in Fig. 2 for a series of times as seen in STEREO-A EIT 304 Å on the NE limb. The orientation of the filament prior to its eruption was nearly parallel with lines of constant latitude. Hence the STEREO-A view is nearly from the west end of the pre-eruptive filament seen against the solar disk. This is an excellent perspective for viewing the rolling motion of the top of the prominence. Prior to its eruption the top of the prominence was nearly vertical above its base. As the top ascended, it also bent southward until the motion of the top is momentarily nearly parallel with the solar surface at 05:46 UT. The rolling motion continued for more than 180°. We are unable to see whether the rolling motion continues after 07:56 UT.

The prominence eruption is not as obviously non-radial as seen at the north-west limb from STEREO-B spacecraft (Fig. 3) because the STEREO-B perspective of the prominence is broadside rather than from one end as for STEREO-A: the separation angle between A and B was 86.7°, which allow to observe the eruption from the two, approximately perpendicular, points of view. Nevertheless, the direction of roll can be recognized and established definitively from the combination of EUVI 304 Å images from the two spacecraft. In the set of images in Fig. 3 from STEREO-B, the roll is toward us as the observers.

It is very clear that the southward rolling motion is accompanied by southward non-radial motion of the overlying corona loop system. As the overlying coronal loops do not participate in the sideways rolling motion of the prominence, we note that the prominence shows a higher degree of non-radial motion than the CME and we suggest this difference is due to its rolling motion. In previous papers on the roll effect (Martin, 2003; Panasenco and Martin, 2008), the associated CMEs were not studied. Therefore, it was not recognized whether the direction of the rolling mass motions could be related to the non-radial motion of the surrounding CME and therefore possibly also related to forces that could cause the whole CME to be non-radial.

The prominence spine prior to eruption was also connected to the disk at each end and also along its sides by threads extending from the filament spine to either side called barbs (Martin, 1998). When a prominence erupts the barbs become detached from the chromosphere. To keep our model of the rolling motion of the prominence simple, we suggest that the barbs threads on opposite sides of the prominence reconnect with each other and collapse back into the spine which retains its ribbon-like topology.

Previously, we have modeled the spine of erupting prominences as flat ribbons that can be bent and twisted (Panasenco and Martin, 2008). We found that the shapes of prominences both before and during eruption could be more closely reproduced by the bending and twisting of a flat ribbon than modeling the prominence mass like a flux tube (Panasenco and Martin, 2008). For this reason, we also empirically model the spine of this erupting filament on December 12, 2008 as a narrow ribbon lying on one edge. The spine is modeled as parallel magnetic threads within the ribbon except where they bend to the chromosphere at their ends. Except at its extreme ends, the ribbon is horizontal and parallel with polarity boundary when it begins to rise slowly prior to its eruption. To create the empirical model of the rolling motion of the prominence spine during the eruption, we first identify the approximate locations of footpoints of the filament at chromosphere in the 304 Å images. Then using the commercial program 3 ds *MAX*, we create a ribbon with the height and length of the filament prior to eruption as seen in 304 Å, (Fig. 4). Next, the model ribbon is distorted in the simplest possible way to match the appearance of the erupting prominence at a given time as seen from the perspective of STEREO-A (Fig. 5a). Then the model Sun with its model prominence is rotated in increments of 18° to show the prominence from different perspectives (Fig. 5b–f). Panel f is the perspective of the empirical prominence model as seen from STEREO-B. We see that our empirical model represents well the outer edge and most of the prominence as seen at STEREO-B. We thus see that our model is useful as a first approximation of the overall topology of the erupting filament.

Since we are able to see the prominence and the CME from both STEREO spacecraft, we can create a three-dimensional representation of both to determine basic spatial information and speeds of parts of the prominence as it erupts. For this purpose, we have used the IDL routine `scc_measure` which employs the tie-pointing technique. Individual features were selected in the prominence mass and in the leading edge of the CME and were traced in most of the images in EUVI 304 Å as well as in the coronagraphs COR1 and COR2 images. A feature in the leading edge was also traced in COR1 and COR2 images. Fig. 6 shows the features in the prominence and in the CME leading edge as seen from COR1 A and B images that were used to carry out the reconstruction. The results from this calculation are shown in the graphs in Fig. 7.

The left panel of Fig. 7 shows the true coordinates of the top of the erupting prominence as seen in EUVI 304 Å observations. The prominence underwent a very gradual rise for more than an hour before its eventual eruption that started at 03:56 UT. This early eruptive phase was also found to be quite slow, its true speed being approximately 50 km/s in the interval from 04:00 to 07:00 UT. A notable change is the decrease in latitude (bottom panel) of the prominence from 47° to 24° once it starts to erupt. Later the prominence, however, was seen to erupt much more rapidly in the coronagraphs COR1 and COR2 images (middle panels), its true speed being around 190 km/s. Whereas a point